Silicon carbide-on-insulator thermal-piezoresistive resonator for harsh environment application

Sun, Baoyun; Mo, Jiarui; Zhang, Hemin ; van Zeijl, Henk W.; van Driel, Willem D.; Zhang, Guoqi

DOI
10.1109/MEMS49605.2023.10052401

Publication date
2023

Document Version
Final published version

Published in
Proceedings of the 2023 IEEE 36th International Conference on Micro Electro Mechanical Systems (MEMS)

Citation (APA)
Sun, B., Mo, J., Zhang, H., van Zeijl, H. W., van Driel, W. D., & Zhang, G. (2023). Silicon carbide-on-insulator thermal-piezoresistive resonator for harsh environment application. In *Proceedings of the 2023 IEEE 36th International Conference on Micro Electro Mechanical Systems (MEMS)* (pp. 621-624). IEEE. https://doi.org/10.1109/MEMS49605.2023.10052401

SILICON CARBIDE-ON-INSULATOR THERMAL-PIEZORESISTIVE RESONATOR FOR HARSH ENVIRONMENT APPLICATION

Baoyun Sun[1, 2*], *Jiarui Mo*[1], *Hemin Zhang*[3*], *Henk W. van Zeijl*[1], *Willem D. van Driel*[1], *and Guoqi Zhang*[1]

[1]Department of Microelectronics, Delft University of Technology, The NETHERLANDS
[2]Department of Engineering Mechanics, China University of Petroleum (East China), CHINA and
[3]Department of Electrical Engineering (ESAT-MNS), KU Leuven, BELGIUM

2023 IEEE 36th International Conference on Micro Electro Mechanical Systems (MEMS) | 978-1-6654-9308-6/23/$31.00 ©2023 IEEE | DOI: 10.1109/MEMS49605.2023.10052401

ABSTRACT

The thermal-piezoresistive effect in silicon (Si) has attracted great attention toward high-performance resonant devices but still faces major challenges for harsh environment applications. Instead of using Si, this paper, for the first time, reports a thermal-piezoresistive resonator based on a silicon carbide-on-insulator (SiCOI) platform. The resonance frequency simulation, CMOS-compatible fabrication, and thermoresistive properties characterization of the proposed SiCOI resonator are presented. The experimental results show linear current-voltage characteristics and a constant temperature coefficient of resistance (TCR) up to 200 °C.

KEYWORDS

Silicon carbide-on-insulator, thermal-piezoresistive, resonator, harsh environment.

INTRODUCTION

Since the first miniature Si piezoresistive heat engine was reported in 2011 [1], a variety of self-sustained thermal-piezoresistive resonators or oscillators have been developed for mass sensing [2, 3], Lorentz force measurement [4], gas detection [5], and signal amplification [6]. It was demonstrated that the thermal-piezoresistive effect is strong enough to initiate and maintain the mechanical oscillation of the resonator driven by direct current (DC), without the demand for any external alternating current (AC) source and amplifying circuitry. Moreover, the self-sustained oscillation enabled by this effect can significantly improve the quality factor of the resonator, resulting in an enhanced signal-to-noise ratio and sensitivity. However, the state-of-the-art thermal-piezoresistive resonators are mainly based on silicon-on-insulator (SOI) microelectromechanical systems (MEMS) technology. Owing to the intrinsic properties of Si, it is a major challenge to implement SOI resonant devices in harsh environments, like high temperatures and pressure, aggressive chemical corrosion, strong electric field, intense radiation, and high shock or vibration.

To overcome the limitations of Si devices, wide bandgap (WBG) semiconductor materials possessing a bandgap of 2.2 eV or higher [7], have recently attracted tremendous attention as possible MEMS platforms for extreme environment applications. Among all the WBG materials, silicon carbide (SiC) is one of the most appealing platforms for hostile environments compatible MEMS devices [8, 9], as its unique combination of excellent electrical, thermal, and mechanical properties. Furthermore, with the rapid progress in massive production and CMOS processing, SiC also enjoys the benefits of commercial availability of high-quality crystalline bulk wafers and compatibility with current CMOS nanofabrication processes.

SiC exists in more than 200 polytypes that are generally categorized into α-SiC and β-SiC [10, 11]. The most common α-SiC crystal structures are the hexagonal SiC including 4H- (bandgap 3.2 eV) and 6H-SiC (bandgap 3.0 eV) which are commercially available up to 200 mm in diameter. 3C-SiC (bandgap 2.3 eV) is the only cubic crystal of SiC, commonly known as β-SiC. As 3C-SiC is the lowest-temperature phase among all the SiC polytypes, it can be epitaxially grown on Si substrates by the chemical vapor deposition (CVD) method [12, 13]. Compared with Si, the large bandgap of SiC dramatically reduced the leakage current at elevated temperatures. The high ratio between Young's modulus and density enables high-frequency MEMS resonators and oscillators. In addition, the high thermal conductivity is especially crucial for quickly heating up and cooling down the beam in the thermal-piezoresistive resonator.

Here, we demonstrated a 3C-SiCOI thermal-piezoresistive resonator based on the internal thermodynamic feedback mechanism. The proposed structure and working principle of the resonator are described. The dependence of the resonance frequency on the piezoresistive beam dimension is determined by finite element analysis. A CMOS-compatible fabrication process for the SiCOI resonator is established. Experimental measurements are performed to characterize the thermoresistive properties of the resonator.

DESIGN AND SIMULATION

To implement the thermal-piezoresistive effect in SiC, we propose a resonator based on a SiCOI platform with a negative piezoresistive coefficient. The SiCOI thermal-piezoresistive resonator is comprised of two symmetrical suspended masses connected by a narrow piezoresistive beam and supported by four spring beams [14]. Figure 1(a) shows the finite element model of the SiC resonator oscillating in its in-plane mode. The two mass plates are free to move back and forth in the in-plane direction. The ends of the four spring beams are kept fixed to obtain eigenfrequency by simulation.

The operation mechanism of the thermal-piezoresistive resonator is attributed to the internal thermodynamic feedback illustrated in Figure 1(b). The device oscillates from its initial state (phase (1)). A constant DC (I_{dc}) passes through the piezoresistive beam, resulting in an increasing beam temperature T_b caused by the resistive heating power $P_h = I_{dc}^2 R_b$. The heat capacitance of the piezoresistive beam leads to a thermal delay between resistive heating power and temperature in the beam. Consequently, the beam expands at a higher temperature, and the strain in the beam is tensile. Meanwhile, the beam resistance decreases due to the negative piezoresistive coefficient. In phase (3), the beam resistance reaches its minimum value. The beam starts cooling and contracts to its initial state. In phase (5), the beam continues to contract because of the beam temperature is reduced, until it reaches phase (7) where the strain is compressive. Finally, the beam is heated and expanded again to phase (1). Thus, the beam expansion/contraction cycle forms an in-plane mechanical vibration. The piezoresistive beam is used as both a thermal actuator and a piezoresistive sensor in this structure. The oscillation of the beam can be detected by the alternating output voltage.

As a result of the geometry of the resonant structure, the heating power density and mechanical strain are concentrated in the narrow piezoresistive beam, but the resonance frequency of the structure is mainly determined by the masses and spring beams. The finite element analysis results shown in Figure 2 suggest that the 3C-SiC thermal-piezoresistive resonator can generate an in-plane mechanical resonance over 1 MHz. The eigenfrequency increases with increasing piezoresistive beam length and width. Scaling down the length-to-width ratio of the beam leads to a higher resonance frequency. Furthermore, scaling the beam dimension down reduces the power consumption of the resonator while having a higher resonance frequency. On the other hand, the effect of the beam thickness on the eigenfrequency can be neglected.

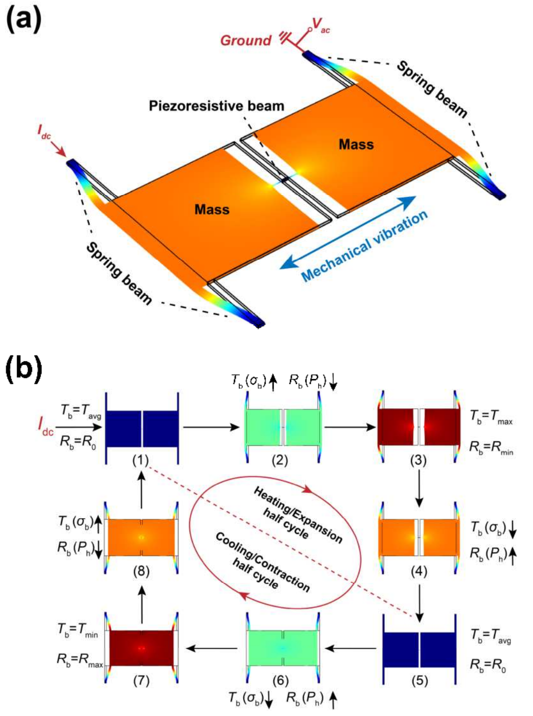

Figure 1: (a) Finite element model of the SiCOI piezoresistive resonator. (b) Schematic illustration of the thermodynamic cycle in the thermo-piezoresistive resonator. The heating power in the piezoresistive beam depends on its position as a result of the piezoresistive effect. Phases (1)-(4) indicate the heating and expansion half cycle, and phases (5)-(8) indicate the cooling and contraction half cycle.

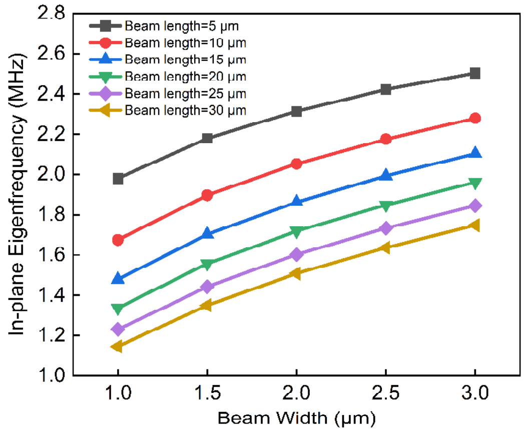

Figure 2: Finite element analysis results of the in-plane resonance frequency change with the piezoresistive beam length and width.

FABRICATION

The fabrication process of the proposed SiCOI thermal-piezoresistive resonator is schematically shown in Figure 3. The process begins with a double side polished 4-inch Si handle wafer with a thickness of 400 ± 8 μm. The Si wafer is thermally oxidized to provide a 2 μm thick buried SiO_2 layer on both sides. The 3C-SiC film is deposited on the Si wafer by low-pressure chemical vapor deposition (LPCVD) at 860 °C and 0.6 Torr. Dichlorosilane (SiH_2Cl_2) and acetylene (C_2H_2) with a flow rate of 80 sccm and 16 sccm are selected as precursor gases, respectively. Ammonia (NH_3) with a flow rate of 1.5 sccm diluted in hydrogen (H_2) is introduced as an N-type dopant during the deposition. As a result, a 1.7 μm thick N-type 3C-SiC film with an average resistivity of 0.02 Ω·cm and a negative piezoresistive coefficient [9] is obtained. The material stack of the created 3C-SiCOI platform is shown in Figure 3(a). The residual stress of the 3C-SiCOI platform is measured to be 6.8 MPa. Such small tensile stress enables flat multilayer thin films without buckling.

Starting with the 3C-SiCOI, the resonator structure is transferred into the top 3C-SiC device layer via lithography and chlorine (Cl_2)/ hydrogen bromide (HBr) plasma etching. A 500 nm thick titanium (Ti) metal layer is then sputtered onto the top 3C-SiC layer at 350 °C to form Ohmic contact with low contact resistance, followed by plasma etching. After finishing the frontside processing, the backside 3C-SiC and SiO_2 layers are opened using plasma etching in two steps. The 3C-SiC and SiO_2 films leave on the backside after etching act as hard masks for the subsequent Si deep reactive ion etching (DRIE). The "Bosch DRIE process" is employed to etch through the Si wafer. In the last step, the frontside SiO_2 layer underneath the resonator structure is removed using vapor hydrogen fluoride (HF) etching. Finally, the suspended 3C-SiCOI thermal-piezoresistive resonator is achieved.

The scanning electron micrograph (SEM) images of the resonator structure are shown in Figure 4. Two 400 μm × 400 μm suspended masses are connected by a 30 μm long, 1 μm wide piezoresistive beam. The masses are supported by four spring beams with the same length of 200 μm and width of 10 μm. Figure 4(b)-(c) show the zoom-in views of the piezoresistive beam and spring beam, respectively.

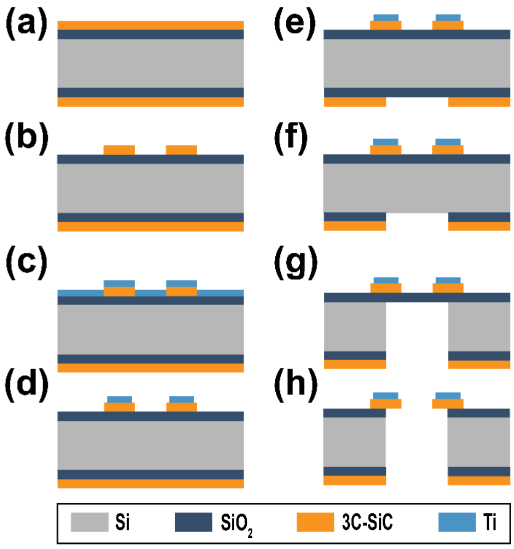

Figure 3: Schematic representation of the industry-standard, CMOS-compatible microfabrication process flow. (a) 3C-SiC thin film deposition and doping by LPCVD. (b) Frontside SiC resonator structure patterning via plasma etching. (c) Metal layer (Ti) deposition. (d) Metal layer patterning. (e) Backside 3C-SiC layer patterning. (f) Backside SiO₂ layer patterning. (g) Through-Si etching lands on the frontside SiO₂ sacrificial layer via the "Bosch process". (h) SiO₂ sacrificial layer removing in vapor HF.

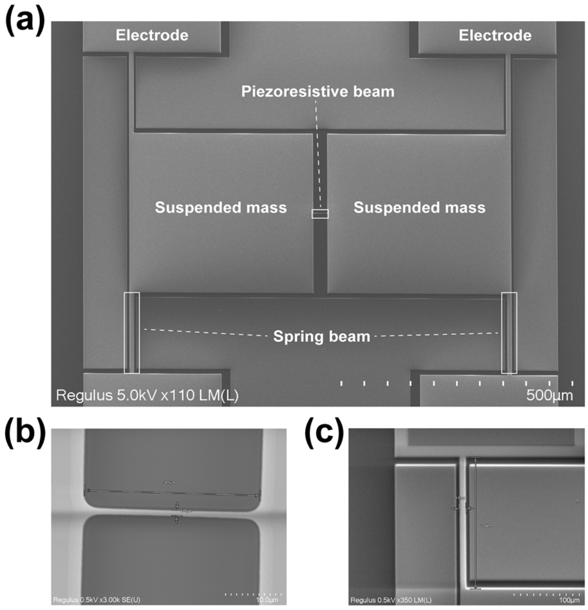

Figure 4: (a) Scanning electron micrograph (SEM) image of the SiCOI thermo-piezoresistive resonator. (b) Magnification of the piezoresistive beam. (c) Magnification of a spring beam.

THERMORESISTIVE CHARACTERISTIC

The thermoresistive effect of the 3C-SiC resonator was characterized by the CascadeMicrotech probe system. The applied current varied from -50 µA to 50 µA. Figure 5 shows the measurement results for the current-voltage (I-V) characteristics of the resonator at various temperatures ranging from 25 °C to 200 °C. The output voltage is linearly increased with the increasing current in the whole temperature range. The linear I-V curves indicate good Ohmic contact between the Ti electrodes and the 3C-SiC film is maintained at elevated temperatures. At a constant applied current, the measured voltage decreased with increasing temperature. The conduction of N-type 3C-SiC is thermally activated.

Figure 6 shows the relative resistance change of the resonator as a function of ambient temperature. The relative resistance change ($\Delta R/R$) linearly decreased with increasing temperature up to 200 °C. According to the definition of temperature coefficient of resistance (TCR),

$$\mathrm{TCR}=(R_T-R_0)/[(T-T_0)\,R_0] \quad (1)$$

where R_T is the resistance at temperature T, and R_0 is the reference resistance at room temperature T_0 (20 °C). The corresponding temperature coefficient of resistance (TCR) value is calculated to be -1670 ppm/°C. The constant TCR is of high interest for MEMS resonators working at elevated temperatures in terms of simplicity in the design and implementation of circuitry.

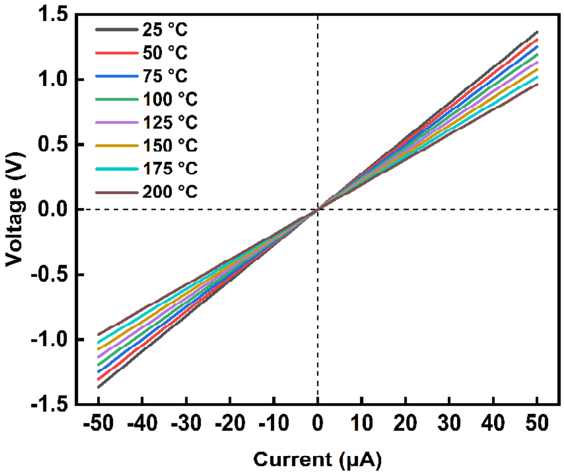

Figure 5: Current-voltage (I-V) characteristics of the 3C-SiC resonator at various temperatures ranging from 25 ℃ to 200 ℃.

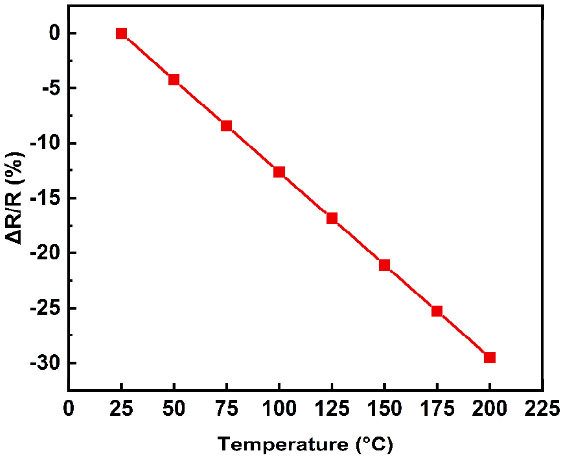

Figure 6: Relative resistance change as a function of the temperature.

CONCLUSION

In summary, we have demonstrated an N-type 3C-SiCOI thermal-piezoresistive resonator for high-temperature applications. The resonator structure design and operation mechanism were introduced in detail. The finite element analysis of the resonator indicates a high in-plane eigenfrequency over 1 MHz. We have developed a CMOS-compatible process for the SiCOI resonator fabrication. The as-fabricated device shows a linear I-V characteristic and constant negative TCR value up to 200 °C. Our work provides a viable route toward harsh environment-compatible, self-sustained SiCOI resonate devices. The thermal-piezoresistive effect at high temperatures and frequency responses of the SiCOI resonator in this work need to be further investigated and tested.

ACKNOWLEDGEMENTS

The authors thank the staff of Delft University of Technology Else Kooi Laboratory (EKL) for processing support. This work is supported by the European Union's Horizon 2020 research and innovation programme under grant agreement No 871741 and No 876659, ITEA-EUREKA project No 19037.

REFERENCES

[1] P. G. Steeneken, K. Le Phan, M. J. Goossens *et al.*, "Piezoresistive heat engine and refrigerator," *Nat. Phys.,* vol. 7, no. 4, pp. 354-359, 2011.

[2] A. Quan, H. Zhang, C. Wang *et al.*, "A Self-Sustained Mass Sensor With Physical Closed Loop Based on Thermal-Piezoresistive Coupled Resonators," *IEEE Trans. Electron Devices,* vol. 69, no. 10, pp. 5808-5813, 2022.

[3] A. Quan, C. Wang, H. Zhang *et al.*, "A Thermal-Piezoresistive Self-Sustained Resonant Mass Sensor with High-Q (>95k) in Air," in *21st International Conference on Solid-State Sensors, Actuators and Microsystems (Transducers)*, June 20-24, 2021, pp. 168-171.

[4] V. Kumar, A. Ramezany, M. Mahdavi *et al.*, "Amplitude modulated Lorentz force MEMS magnetometer with picotesla sensitivity," *J. Micromech. Microeng.,* vol. 26, no. 10, 2016.

[5] X. Guo, Y.-b. Yi, and S. Pourkamali, "Thermal-Piezoresistive Resonators and Self-Sustained Oscillators for Gas Recognition and Pressure Sensing," *IEEE Sens. J.,* vol. 13, no. 8, pp. 2863-2872, 2013.

[6] A. Ramezany, M. Mahdavi, and S. Pourkamali, "Nanoelectromechanical resonant narrow-band amplifiers," *Microsyst. Nanoeng.,* vol. 2, pp. 16004, 2016.

[7] M. N. Yoder, "Wide bandgap semiconductor materials and devices," *IEEE Trans. Electron Devices,* vol. 43, no. 10, pp. 1633-1636, 1996.

[8] J. Romijn, S. Vollebregt, L. M. Middelburg *et al.*, "Integrated 64 pixel UV image sensor and readout in a silicon carbide CMOS technology," *Microsyst. Nanoeng.,* vol. 8, pp. 114, 2022.

[9] L. M. Middelburg, H. W. van Zeijl, S. Vollebregt *et al.*, "Toward a Self-Sensing Piezoresistive Pressure Sensor for All-SiC Monolithic Integration," *IEEE Sens. J.,* vol. 20, no. 19, pp. 11265-11274, 2020.

[10] C. Eddy, and D. Gaskill, "Silicon carbide as a platform for power electronics," *Science,* vol. 324, no. 5933, pp. 1398-1400, 2009.

[11] A. L. Falk, B. B. Buckley, G. Calusine *et al.*, "Polytype control of spin qubits in silicon carbide," *Nat Commun,* vol. 4, pp. 1819, 2013.

[12] C. A. Zorman, A. J. Fleischman, A. S. Dewa *et al.*, "Epitaxial growth of 3C–SiC films on 4 in. diam (100) silicon wafers by atmospheric pressure chemical vapor deposition," *J. Appl. Phys.,* vol. 78, no. 8, pp. 5136-5138, 1995.

[13] L. Wang, S. Dimitrijev, J. Han *et al.*, "Growth of 3C–SiC on 150-mm Si (100) substrates by alternating supply epitaxy at 1000 °C," *Thin solid films,* vol. 519, no. 19, pp. 6443-6446, 2011.

[14] H. Zhang, A. Quan, C. Wang *et al.*, "A Fast-Startup Self-Sustained Thermal-Piezoresistive Oscillaror with >10^6 Effective Quality Factor In the Air," in *IEEE 35th International Conference on Micro Electro Mechanical Systems Conference (MEMS)*, January 9-13, Tokyo, 2022, pp. 142-145.

CONTACT

*Baoyun Sun, b.sun-3@tudelft.nl
*Hemin Zhang, 1989hemin@gmail.com